LBNL-39277
UC-410

ERNEST ORLANDO LAWRENCE
BERKELEY NATIONAL LABORATORY

Some New Schemes for Producing High-Accuracy Elliptical X-ray Mirrors by Elastic Bending

H.A. Padmore, M.R. Howells, S. Irick,
T. Renner, R. Sandler, and Y.-M. Koo
Accelerator and Fusion Research Division

August 1996
Presented at the *SPIE Conference*, Denver, CO, August 5–9, 1996, and to be published in the Proceedings

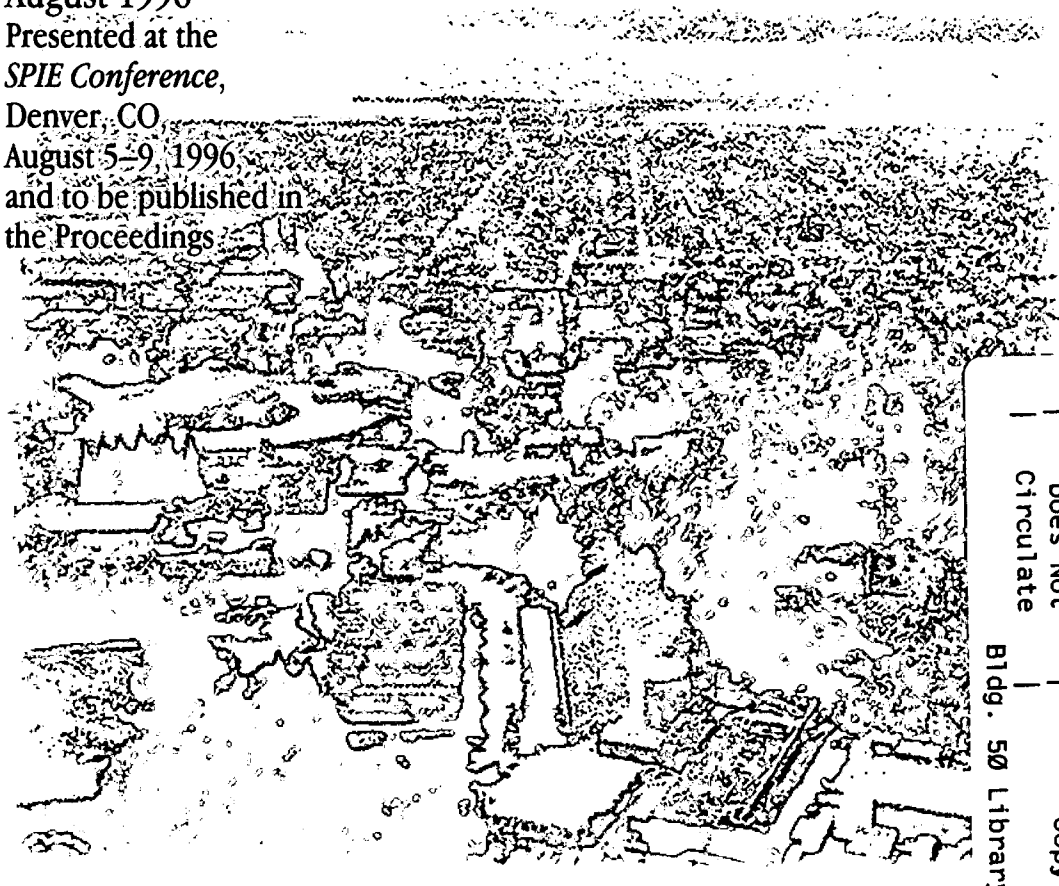

DISCLAIMER

LBNL-39277
LSBL-347
UC-410

SOME NEW SCHEMES FOR PRODUCING HIGH-ACCURACY ELLIPTICAL X-RAY MIRRORS BY ELASTIC BENDING*

H.A. Padmore, M.R. Howells, S. Irick, T. Renner, R. Sandler
Advanced Light Source, Lawrence Berkeley National Laboratory
University of California, Berkeley, California 94720

Y.-M. Koo
Department of Materials Science and Technology
Pohang University of Science and Technology
San 31 Hyoja Dong, Pohang, Kyungbuk, 790-784
Republic of Korea

To be published in SPIE 2856, Optics for High Brightness
Synchrotron Radiation Beamlines II, Denver, August 1996

*This work was supported by the Director, Office of Energy Research, Office of Basic Energy Sciences, Materials Sciences Division, of the U.S. Department of Energy, under Contract No. DE-AC03-76SF00098.

Some new schemes for producing high-accuracy elliptical x-ray mirrors by elastic bending

H. A. Padmore[1], M. R. Howells[1], S. Irick[1], T. Renner[1], R. Sandler[1] and Y-M. Koo[2]

[1]Advanced Light Source, Accelerator and Fusion Research Division,
Lawrence Berkeley National Laboratory, Berkeley, CA 94720, USA
[2]Pohang University of Science and Technology, Pohang 790-784, Republic of Korea

ABSTRACT

Although x-ray micro-foci can be produced by a variety of diffractive methods, grazing incidence mirrors are the only route to an achromatic focus. In this paper we describe our efforts to produce elliptically shaped mirrors with the very high figure accuracy necessary for producing a micro-focus. The motivation for this work is provided by the need to produce achromatic foci for a range of applications ranging from tunable micro-focus x-ray photoelectron spectroscopy (μ-XPS) at soft x-ray energies to micro-focus white beam x-ray diffraction (μ-XRD) at hard x-ray energies. We describe the methodology of beam bending, a practical example of a system we have produced for μ-XRD, and results demonstrating the production of a surface with micro-radian figure accuracy.

Keywords: Synchrotron radiation, mirrors, adaptive, x-ray, microprobe

1. INTRODUCTION

Substantial progress has been made in recent years in the fabrication of low slope error x-ray mirror surfaces by controlled grinding and polishing. One of the motivations for this improvement has been the advent of 3rd generation synchrotron radiation sources which have given many orders of magnitude increase in brightness over older machines, and have enabled many new types of microscopy and microanalysis to be performed.

We report here on progress in developing bendable mirror technology, and its application to probe-forming optics for x-ray imaging systems at the Advanced Light Source. We have adopted this approach over conventional rigid-mirror technology partly as a cost saving measure and partly to simplify the production of aspheric surfaces. The cost advantage follows from the use of *flat* polishing while the desire for aspheric surfaces comes from the need to operate grazing-incidence mirrors with a combination of high demagnification and large aperture in order to form high intensity focal spots in the micron range.

The approach that we describe here is to bend a constant-thickness metal or ceramic mirror by the application of unequal end couples. If the mirror has a constant width as well a constant thickness, then the result is a cubic curve which can be made to approximate an ellipse up to third order which enables correction of defocus and coma[1] while leaving higher-order aberrations uncorrected. Higher order corrections to the bent shape are made, if required, by applying a programmable

variation to the mirror width. Techniques of this general type have often been used before for both normal[2] and grazing-incidence[3-5] systems and have been quite widely used for focusing synchrotron radiation[6,7,8] including the use of bent metal mirrors with water cooling[9] and directly-deformable piezo-ceramic mirrors[10]. The programmable-width concept was first introduced by Underwood and collaborators[1] while the Advanced Light Source (ALS) group have developed a variable-thickness scheme in which the mirror and bending mechanism are built into a single monolith[11,12]. The situation as of 1993 was reviewed by Howells and Lunt[12].

Some of the above-mentioned mirrors have achieved their specified performance levels while others have failed due to the application of unintended additional forces by the mechanism used to apply the couples. The difficulty of applying the couples with sufficient accuracy is increasing at the present time due to the smaller focal spots that are being sought. In this paper we describe some new ways to apply the couples via weak leaf springs. This approach makes it much simpler to control the amount of bending with high accuracy and also lends itself to schemes that do not apply tensile forces to the mirror. We will concentrate specifically on elliptical mirrors used for forming fine x-ray microprobes which implies relatively small mirrors but the methods of construction we will discuss are applicable to a wider class of optics. Test results using a long trace profiler indicate that micro-radian tolerances are being achieved with these techniques.

2. GEOMETRY OF AN ELLIPSE

When we build an aberration-corrected mirror we are trying to approximate the elliptical cylinder $X^2/a^2 + Y^2/b^2 = 1$ whose section is shown in Fig. 1. Such an ellipse can be represented by a power series in the x, y coordinates of Fig. 1 as follows;

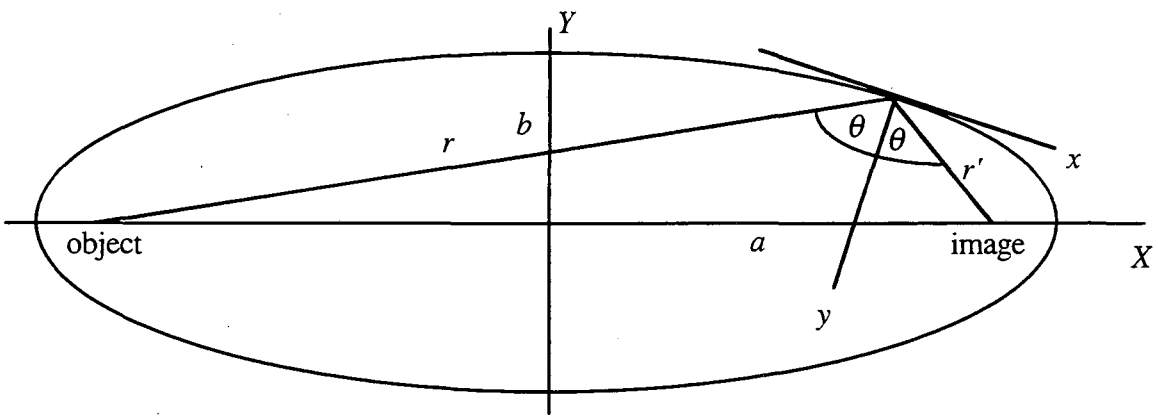

Fig. 1. Ellipse layout and notation.

$$y = a_2x^2 + a_3x^3 + a_4x^4 + \ldots \tag{1}$$

of which the curvature is,

$$\frac{d^2y}{dx^2} = 2a_2 + 6a_3x + 12a_4x^2 + \ldots \tag{2}$$

The a_i's for the ellipse are given by,

$$a_2 = \frac{\cos\theta(r+r')}{4rr'} = \frac{1}{2R_0}$$
$$a_3 = -a_2\frac{\sin\theta}{2}\left(\frac{1}{r}-\frac{1}{r'}\right) \tag{3}$$
$$a_4 = a_2\left(\frac{5\sin^2\theta}{16}\left(\frac{1}{r}-\frac{1}{r'}\right)^2+\frac{1}{4rr'}\right)$$

where R_0 is the center radius of the mirror. Each term $a_i x^i$ of the series in eq. (1) corresponds to an aberration which will be corrected if the term is faithfully built into the mirror shape. The i=2 term corresponds to defocus, the i=3 one to coma[13] (linear variation of curvature with position in the aperture (see eq. (2)) the i=4 one to spherical aberration (quadratic variation of curvature with position in the aperture) and so on.

The major and minor semiaxes, a and b and eccentricity e of the ellipse and the coordinates (X_0, Y_0) of the pole of the mirror are related to the optical parameters r, r' and θ by the following relations,

$$2a = r+r' \qquad Y_0 = \frac{rr'\sin 2\theta}{2ae}$$
$$(2ae)^2 = r^2+r'^2-2rr'\cos 2\theta$$
$$b^2 = a^2\left(1-e^2\right) \qquad X_0 = \pm a\sqrt{1-\frac{Y_0^2}{b^2}}$$

where the square root is +, zero or - according as $r >, =$ or $< r'$.

3. FORMATION OF AN ELLIPTICAL SURFACE BY BEAM BENDING

First consider a beam that is being bent by the action of two end couples C_1 and C_2 defined to be positive in the sense drawn in Fig. 2. One can show that the bending moment will vary linearly from C_1 at x=-L/2 to C_2 at x=+L/2. The differential equation for the shape of the bent beam is the Bernouilli-Euler equation[14] which now takes the following form,

$$EI_0\frac{d^2y}{dx^2} = \frac{C_1+C_2}{2} - \frac{C_1-C_2}{L}x \tag{4}$$

where E is Young's modulus and I_0 is the moment of inertia of the beam cross section, considered for the moment to be constant. The applied stress at each beam end is assumed to have a linear variation in y with a zero at the neutral axis and a resultant moment C_1 or C_2.

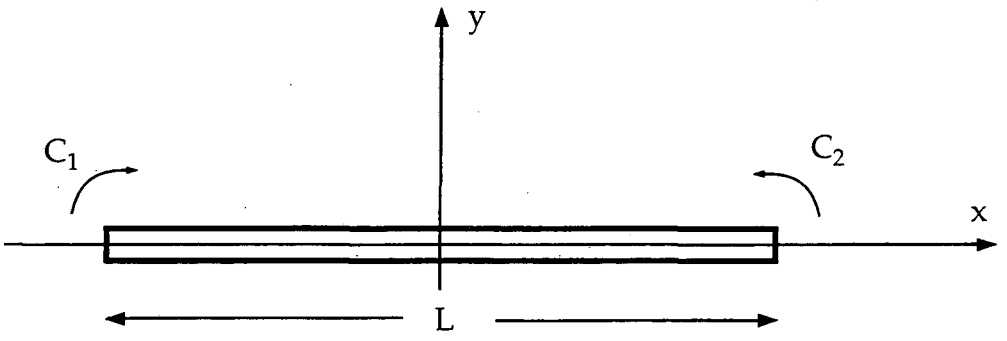

Fig 2. Nomenclature for discussing beam bending using two couples

In order to make the cubic approximation to the ellipse (i=2 and 3 terms of eq. (1)),we equate coefficients of the constant and linear terms of eqs. (2) and (4) to obtain the required values of C_1 and C_2.

$$C_1 + C_2 = 4EI_0a_2 = \frac{2EI_0}{R_0} \tag{5}$$

$$C_1 - C_2 = -6EI_0La_3 = \frac{3EI_0L}{R_0}\frac{\sin\theta}{2}\left(\frac{1}{r} - \frac{1}{r'}\right) \tag{6}$$

Such an approximation is often useful and can always be made to satisfy a given aberration tolerance if the mirror aperture is sufficiently reduced. This analysis shows that *bending moment* values C_1 and C_2 at -L/2 and +L/2 can be chosen to deliver this mirror shape within the accuracy of the analysis based on eq. (4). However, the actual couples applied to the mirror need not be positioned at -L/2 and +L/2 and in fact they are best placed somewhat further from the mirror center so as to allow the effect of end errors (imperfect realization of the assumed end-stress distribution) to decay.

Now suppose that we wish to construct a nominally exact elliptical shape using the same applied couples C_1 and C_2 that we calculated for the cubic approximation. We can do this by modifying the width of the mirror so that I_0 in eq. (4) becomes $I(x)$ and is programmed to give the right radius of curvature as specified by eq. (2). Inserting eqs. (5), (6) and (2) into (4) and remembering that $I = bh^3/12$ where b and h are the width and thickness of the mirror respectively, we finally obtain an expression for the width needed to produce the elliptical shape,

$$b(x) = \frac{b_0\left(\frac{1}{R_0} + 6a_3x\right)}{2a_2 + 6a_3x + 12a_4x^2 + \ldots} \tag{7}$$

This approach to producing an elliptical shape differs only slightly from the original one of Underwood[1] in which equal couples were used. The advantage of using unequal couples is that the amount of width variation is generally much less so that the mirror remains approximately rectangular which is convenient for engineering. For cases where the convergence angle from the mirror is a significant fraction of the angle of grazing incidence, terms higher than 4th order have to be included in the surface figure, and to include enough terms in (7) can become difficult. In order to calculate $b(x)$ for a perfect ellipse, the equation of the mirror can be transformed back to the canonical system and the exact curvature can be inserted into eq. (4).

4. USE OF WEAK LEAF SPRINGS FOR BENDING MIRRORS: GENERAL PRINCIPLES

We consider here two types of bending machines: those which put the mirror in tension and those which do not. This can be an important issue because, when tensile forces are present, they tend to straighten the mirror and the error produced may not be negligible. To estimate the size of the error consider a circularly bent mirror with equal couples applied by forces F and bending levers of length l at the ends of the mirror (Fig. 3). This leads to C_1=C_2=Fl and the mirror is subjected to a tensile force F. Allowing for the latter, eq. (4) becomes,[15, 16]

$$\frac{d^2y}{dx^2} - q^2y = q^2l \quad \text{where} \quad q = \sqrt{\frac{F}{EI_0}} \tag{8}$$

leading to a slope distribution,

$$\frac{dy}{dx} = \frac{x}{R_0}\left[\frac{\sinh qx}{qx}\right]. \tag{9}$$

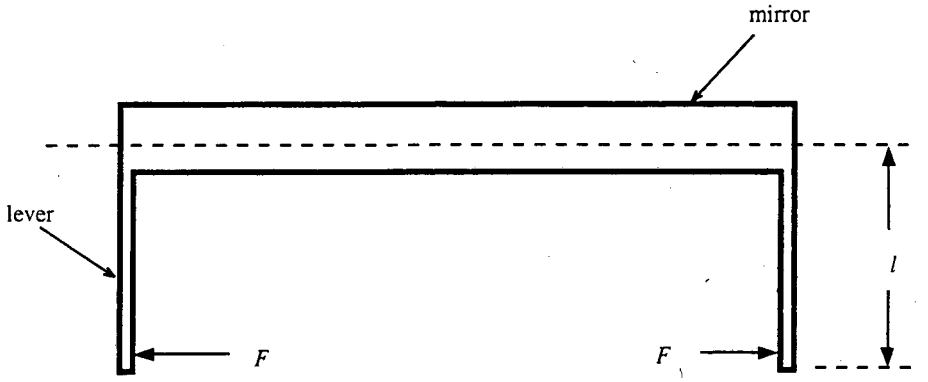

Fig. 3 Mirror in tension due to generation of couples by application of force on a lever

The first term x/R_0 is the slope distribution of the correct circular curve while the term in the square brackets is an error term caused by the tensile force F. When F ends toward zero, the error term tends toward unity. The error is most damaging for long mirrors with steep curvature and short bending levers. For example with L=1 m, l=0.05 m, R_0=100 m, the maximum slope error would be 16 arcseconds. For many practical cases the error may also be negligible (<0.1 arcsecond say).

Example implementations of the two classes of leaf-spring bending mechanisms (with and without the tensile force) are shown in simplified form in Fig. 4. For the majority of cases, the scheme with the tensile force (Fig. 4a) is acceptable and allows somewhat more convenient designs.

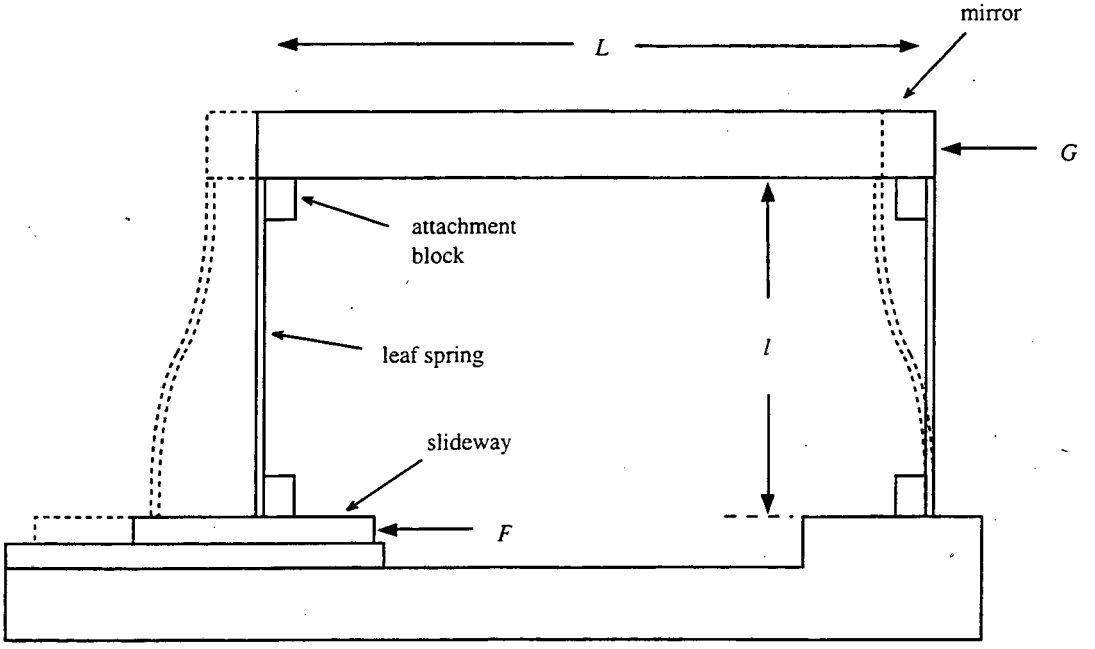

(a)

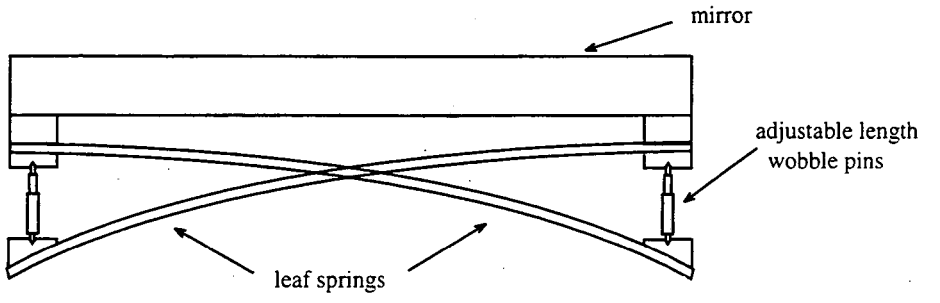

Fig. 4. (a) shows an 's' spring bender in which equal couples are applied by moving the slideway to the left (F), and positive and negative couples are added to the right and left ends respectively by the action of pushing the whole mirror to the left (G). (b) avoids the beam tension implicit in (a) by applying the couples with crossed leaf springs.

To understand the statics of the arrangement suppose the loading is applied in two steps:

Step 1: the force F is applied by moving the slide to the left. This applies couples of *opposite* sense at the mirror ends while the axial forces in the springs remain equal to zero. The magnitude (C) of the couples is $Fl/2$ if the springs are built in at the base as shown. (It would be Fl if they were hinged.)

Step 2: the force G is applied at the right end of the mirror. This applies couples of the *same* sense at the mirror ends while the axial forces in the springs become equal in magnitude and opposite in sign, the one in the right spring being tensile. The magnitude (ΔC) of the applied couples is $Gl/4$ and that of the axial forces is $GL/2l$.

The net effect of these two steps is that couples of magnitude $C+\Delta C$ and $C-\Delta C$ are applied at the right and left ends of the mirror respectively. The value of C, the mean of the two couples, determines the center radius of the mirror (eq. (5). The value of ΔC determines the amount of coma correction (eq. (6). Thus the focal length of the mirror and the amount of aberration correction are *independently* adjustable using F and G.

The advantages of this type of design may be listed as follows:

- There is independent control of focal length and aberration correction.
- The springs are made *weak* so that small deformations of the mirror can be produced by large, and therefore easily controllable, movements of the drivers.
- The use of a prescribed *driving force*, rather than a prescribed *displacement*, allows manufacturing errors or changes in the mirror size (due to thermal expansion for example) to be tolerated as long as they are small compared to the driver motion needed to bend the mirror.
- The forces are applied relative to a rigid base.
- In situations where adhesives can be used the method works for ceramics such as glass and silicon which are required for multilayer substrates.

The crossed-spring bending system shown in Fig. 4b is a variant which does not put the mirror in tension. The springs can easily be designed to cross over without losing symmetry. The scheme has the virtue of simplicity although it lacks the

separation of focusing and aberration correction and does not, in the form shown, have a rigid base, although that can be contrived. Otherwise it shares most of the features of the parallel-spring system.

Both of these systems are being used for mirrors at the ALS . The 's' spring type is being used for μ-XRD and μ-XPS systems, and the crossed-spring type is being used for a 1m long 10:1 demagnifying mirror for soft x-ray photoelectron emission microscopy (PEEM). In the following sections we discuss the case of μ-XRD in detail.

5. A MIRROR BENDER FOR μ-XRD

For x-ray diffraction, we wish to produce an x-ray focus for energies up to 12 KeV, and this dictates the use of a small grazing incidence angle. Assuming a gold coating, adequate reflectivity is achieved for a grazing angle of 1/3°. The synchrotron source is 31 m from the x-ray hutch used for the micro-diffraction experiments (beamline 10.3.2), and our vertical source size of around 30 μm full width at half maximum (FWHM) requires us to use a demagnification of 60:1 to reach our aim of a sub-micron focused beam size. The maximum convergence of the light onto the sample is simply limited by the critical angle of reflection for the highest energies that are required. If a higher convergence angle is used it simply means that, at one end of the mirror, light will be traveling almost parallel to the surface and at the other it will be exceeding the critical angle and will not be reflected. A general rule is that the maximum convergence is half the critical angle. The convergence is related to the acceptance aperture by the demagnification, and so in this case we see that the allowed acceptance is around 50 μrads. At 1/3° grazing incidence angle this equates to a mirror length of 260 mm. In this case however, we limited the optical length to 150 mm.

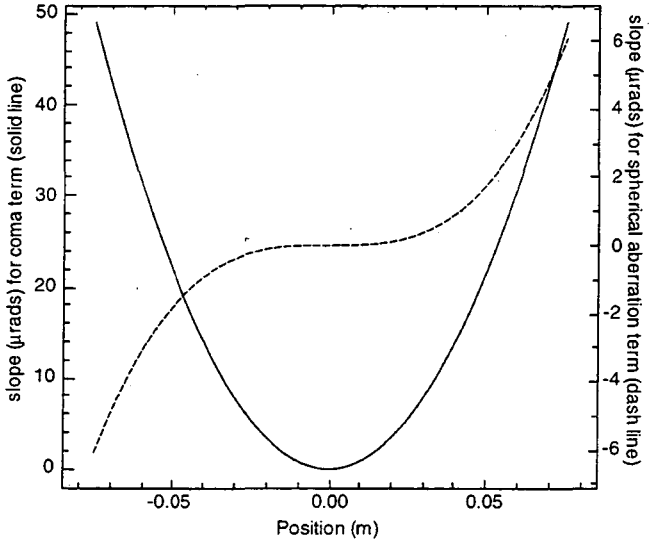

Fig. 5. Coma and spherical aberration contributions to figure error for a circle. Object distance = 31m, image distance = 0.5 m, grazing angle 1/3°

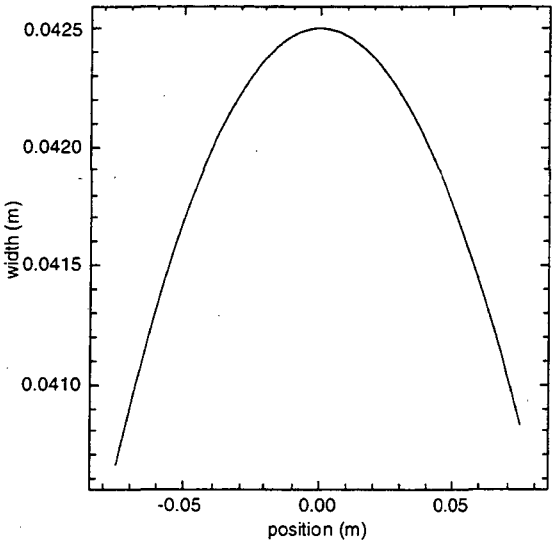

Fig. 6. Width of the beam required to produce an elliptical shape with the parameters give in Fig. 5.

If we take the first derivative of eq. (1), we have the slope as a function of the tangential coordinate along the mirror, x. If we build a mirror system that satisfies only part of the surface expansion, the absent components represent aberrations. For example, if we design an equal couple bender for a mirror of constant width and thickness, only the $2a_2x$ term is present, and the missing higher terms represent aberration. For our chosen parameters above, Fig. 5 shows the slope error contributions for coma ($3a_3x^2$) and spherical aberration ($4a_4x^3$) The marginal-ray coma is 50 μrads, and is symmetric about $x=0$. This symmetry is due to the x^2 variation of the ray aberration. For our image distance of 0.5 m, and remembering that the ray error is doubled on reflection, the extreme rays in a focus would be deviated by 50 μm which is clearly well outside our design target of a 1 μm focus, and must be eliminated. Marginal-ray spherical aberration is ± 6 μrads, and therefore the extreme rays in the image plane would be deviated by ± 6 μm. Again this is unacceptable, but it should be noted that due to the x^3 dependence of the aberration, restricting the aperture to around 1/3 of its full value about $x=0$ would results in a focus size of less than 1 μm.

To correct these and higher order errors, unequal couples and variation of width are used, and in this case, the required width function is shown in Fig. 6. The sum and difference of couples are $C_1+C_2 = 2.65$ N.m and $C_1-C_2 = 0.59$ N.m, for a glass beam of central width 42.5 mm, thickness 9.525 mm, length 150 mm, and Youngs modulus of $7.32\text{x}10^{10}\text{N/m}^2$. Note that the required shaping is modest, varying from 40.6 mm through 42.5 mm to 40.8 mm.

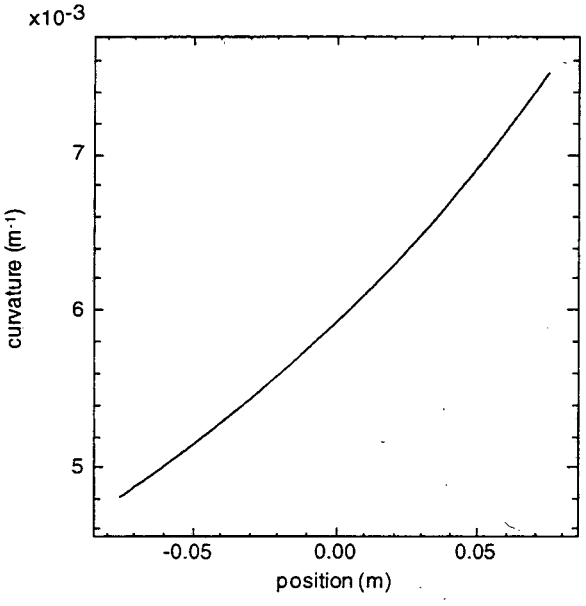

Fig 7. Curvature as a function of position for the mirror defined in Fig. 5

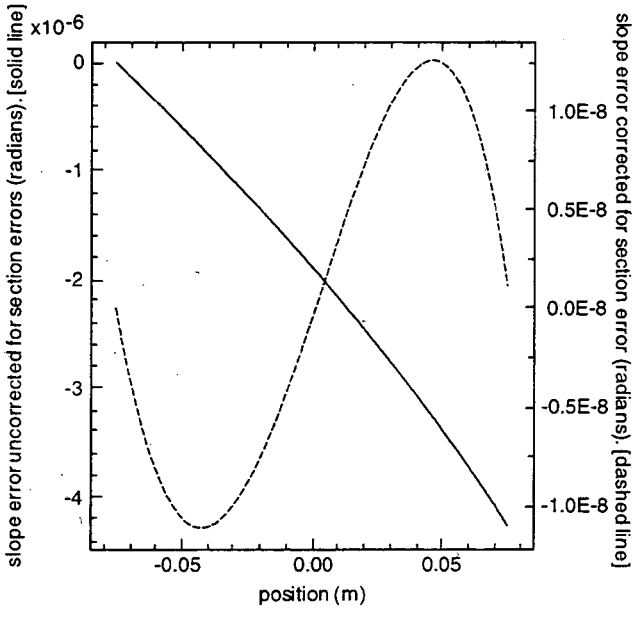

Fig. 8. Solid line shows the figure error resulting from a constant width error of 0.2 mm. Dotted line shows the minimization of the error by adjustment of C_1 and C_2.

The elliptical shape produced has a wide range of curvature, ranging from 0.0048 m^{-1} at one end to 0.0076 m^{-1} at the other, as shown in Fig. 7. In practice errors will occur in several of the mirror parameters, and it is important to understand their

effect, and the extent to which they can be corrected. It can be seem from (5) and (6) that C_1+C_2 and C_1-C_2 are directly proportional to Youngs modulus, E. A fixed change in E is therefore simply accounted for by a change in applied couples. It can also be seen from (7) that a fractional change in width only requires a constant offset of the applied couples to be fully corrected. However, a fixed error in width causes a real error, and an example for a 0.2 mm increase in the width is shown in Fig. 8. The solid line shows the error assuming the original couples are maintained, and the dotted line shows the residual error after adjusting the couples. In this case C_1+C_2 and C_1-C_2 were increased by about 4.8%. Before minimization the error is too large at 4 μrads, but after minimization becomes insignificant. The degree to which correction can be made depends on the extent of the edge shaping. In this case there is only a small fractional width change and couple adjustment is effective. Note that the assumed error is constant. In reality errors will be random or cyclic and in both cases their effect cannot be directly compensated. Errors with a periodicity less than the beam thickness are averaged out, while errors of a significant fraction of the beam length can have a large effect. From a measurement of the manufactured width profile, the error can be directly calculated from eq. (4), putting in the measured value of $I(x)$ and comparing the curvature to that of a perfect ellipse. In our case, our measurements indicate a mean error of +15 μm, with a standard deviation of around 7 μm. This gives an error of less than 0.1 μrads. A more serious error can occur due to variations in thickness. The error can be serious because the dimension of the beam is small in that direction thus increasing fractional errors, and the local curvature scales as the cube of the thickness. In this case, the surface figure accuracy translates into a wedge tolerance along the beam of less than 3 μm, and is easily met. In practice the most common error is wedge, but random or cyclic errors can occur and are much more damaging. This is especially a problem in very thin mirrors.

6. MEASUREMENTS ON THE μ-XRD VERTICAL FOCUS MIRROR

A bending mechanism of the type shown in Fig. 4(a) was constructed for the μ-XRD project. We procured two glass flats fabricated in quartz glass[17] 9.525 mm thick, 42.5 mm wide and 200 mm long. These had sub-μrad flatness as measured with a Long Trace Profiler (LTP)[18] and around 2Å rms roughness measured with a Micromap optical profiler. Steel blocks 10mm in length were glued to the underside of the ends of the mirror using epoxy[19]. The springs of size 0.64 x 50 x 50 mm^3 were deflected approximately 5 mm to produce a central radius of curvature (x=0) of 150 m. Initially we used a full length beam (200 mm) bent with equal couples to test the perfection of bending to a circular shape. The result of this measurement is shown in Fig. 9. The slope of the surface was measured with the LTP, and the data were detrended for tilt, piston and curvature. Fig. 9 shows the residuals for 2 cases; the solid line for the nominally unbent state (920 m radius of curvature) and the dotted line for bending to a radius of 151 m. The latter approximately corresponds to the central radius needed for μ-XRD. It can be seen that these two slope error residuals are almost the same. The difference is shown by the dots, and is essentially zero within the noise of this LTP measurement (<1μrad rms). The conclusion from this is that the mechanism is providing near perfect bending.

It can also be seen that the slope error in both cases is only zero in a central region of ± 20 mm. Outside this region the error increases positively and negatively to the right and left hand sides respectively. This represents an unacceptable error, but not one that is caused by bending. Note that the last few points at each end correspond to an overlap with the areas

in which the blocks are glued to the underneath of the beam, and of course, we do not expect these areas to bend into the desired shape. Even so, the error outside these regions reaches values of ± 20 μrads. The cause of this error is glue shrinkage. Shrinkage causes compression in the underside of the beam, and an extended alteration in the stress distribution. The corresponding strain field cannot be purely local to the glued area, and propagates down the rest of the beam, causing a figure error. In curing, the glue first forms a strong bond, and then over around 12 hours shrinks to a fixed and stable material. We have measured this process in tests using thin silicon wafers, recording the curvature of the surface as a function of time. Most epoxy materials have similar shrinkage values of around 0.4%, but there is some variation in the effect of this shrinkage determined by whether the bond has reached strength before or after shrinkage occurs. However, even with the best materials (around a factor of 2 better than shown here), the shrinkage is a serious problem.

In the present example, the mirror is thick enough (9.525mm) for us to glue the attachment blocks on the end of the beam. In this way, compression given by shrinkage of the glue gives a compressive stress in a direction *perpendicular* to the beam. This is normal to the stresses in the beam which cause bending and hence almost no glue shrinkage induced bending can occur.

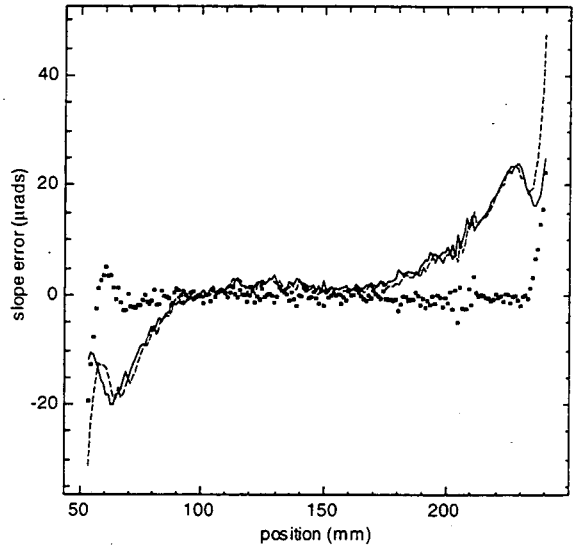

Fig. 9. Solid line shows the slope error from a 920 m radius circle, dotted line shows the error from a 151 m radius, and the dots show the difference

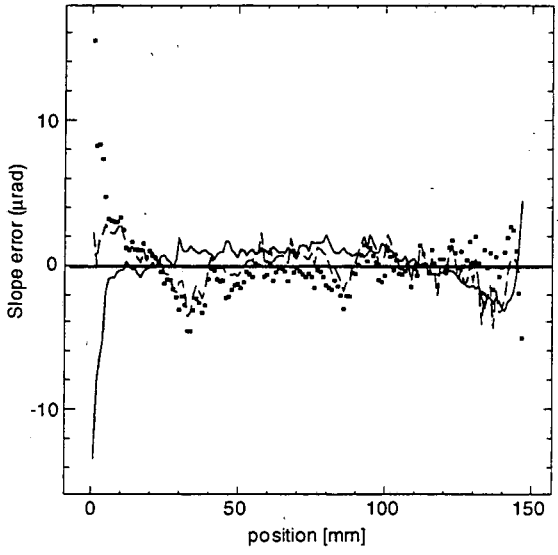

Fig. 10. Solid line gives the slope error of the unbent surface from a flat, the dotted line shows the error from the defined ellipse, and the dots give the difference.

In our second test of the bender system, we shaped the width of the glass beam to the values given in Fig. 6, in addition to gluing the blocks on the ends of the beam. This was performed by CNC machining two steel plates doweled together to the desired shape, and mounting the glass between them on a temporary wax fixture. The plates were used as a template and by careful hand grinding, the glass was machined to the desired shape with a mean error of only 15 μm, resulting in insignificant slope errors. In this case a beam of 170 mm length was used, with a free optical aperture of 150 mm. The measurements on this mirror are shown in Fig. 10. The line shows the deviation from a flat surface, the dotted line shows

the deviation from a best fit ellipse (object distance 31 m, image distance = 0.5 m, grazing angle = 1/3°), and the dots show the difference between the two. The previously flat surface now has a negative error at the left hand side, and a small positive error at the right hand side. The cause of this error turns out to be related to the compressive strain exerted by the bolts used to hold the springs to the attachment blocks. This can be eliminated by introducing a strain relief slot between the end of the bolt and the part of the block used for gluing to the mirror. This is being incorporated into the next iteration of this design, and should entirely eliminate the problem. From the dotted line in Fig. 10, it can be seen that the end effects due to the compression produced by the bolts has been reduced, possibly due to the tensile force in the beam under bending, and that the overall error over the whole length is small. The standard deviation of this error is 1.2 μrads. The dots give the difference between the two curves, and gives an indication of the perfection of bending from flat. These are initial measurements and to save time, the normal averaging and stabilization procedures to get low noise LTP traces were not used. As a result, undoubtedly some of the structure and noise seen in Fig. 10 is instrumental.

7. CONCLUSIONS

We have shown that μradian figure tolerance elliptical optics can be produced by controlled bending of flats. This opens the way to micron or sub-micron white light focusing for application in a wide range of areas. An application that we are currently pursuing is that of μ-XPS. This is a much more demanding case as the radius of curvature is far less (R_0 around 7 m), and therefore to keep the stress at acceptable levels, the beam is much thinner (2 mm) than the example described here. This is difficult for a number of reasons. Thin substrates are flexible, and during polishing will deform with applied pressure. This means that it is difficult to produce thin flats to the required figure accuracy, and front-back surface parallelism. At the same time, parallelism becomes more important as the fractional errors are increased due to the reduced thickness. In addition, as stress is proportional to thickness and inversely proportional to radius of curvature, it can be seen that for the 2 mm thick mirrors for μ-XPS (R_0=7m), in comparison to the 9.525 mm thick μ-XRD mirror described here (R_0=171m), the stress will be 5 times higher. The value of the stress is high enough that care has to be taken to remove cracks and defects caused by the glass machining process by a combination of acid etching and mechanical polishing. It should be noted however that the μ-XRD mirror has suffered several machining operations without apparent problems. In addition, the width profiling did not cause any apparent change in the flatness of the material. One solution to the problem of producing mirrors with small radii of curvature is to produce them in a high strength material, such as steel. This means that the material can be thicker than glass, and together with the higher elastic modulus of steel, the material is much stiffer for polishing. In addition, it can be width profiled in a simple manner by wire electric discharge machining, or CNC milling. We are pursuing the use of both materials for our μ-XPS mirrors. Finally it should be noted that if we obtain a substrate from an optics vendor that has a surface figure and parallelism that are out of specification, so long as we know what these values are, using eq. (4) we can calculate the appropriate width variation to eliminate the error. A further way to achieve the same result is to bend the substrate to the best approximation to the desired elliptical shape, evaluate the error, and calculate the correction in the width necessary to correct the error. The feasibility of such an approach is currently being evaluated.

Acknowledgments

This work was supported by the Director, Office of Energy Research, Office of Basic Energy Sciences, Materials Sciences Division of the U.S. Department of Energy, under Contract no. DE-AC03-76SF00098.

References

1. Underwood, J. H., "Generation of a Parallel X-ray Beam and its use in Testing Collimators", *Space Sci. Instrum.*, **3**, 259-270 (1977).

2. Lemaitre, G., "Optical Figuring by Elastic Relaxation Methods", in *Current Trends in Optics*, Arrecchi, F. T., F. R. Aussenegg, (Ed), Taylor and Francis, London, 1981.

3. Ehrenberg, W., "The Production of Converging Beams by Total Reflection", *J. Opt. Soc. Am.*, **39**, 741-6 (1949).

4. Franks, A., *Brit. J. Appl. Phys.*, **9**, 349-352 (1958).

5. Franks, A., P. R. Breakwell, "Developments in Optically focussing Reflectors for Small-angle X-ray Scattering Cameras", *J. Appl. Cryst.*, **7**, 122-5 (1974).

6. Bilderback, D., C. Henderson, C. Prior, "Elastically Bent Mirror for Focussing Synchrotron X-rays", *Nucl. Inst. Meth.*, **A246**, 428-433 (1986).

7. Heald, S. M., "Applications of Bent Cylindrical Mirrors to X-ray Beams", *Nucl. Inst. Meth.*, **195**, 59-62 (1982).

8. Howell, J. A., P. Horowitz, "Ellipsoidal and Bent Cylindrical Condensing Mirrors for Synchrotron Radiation", *Nucl. Inst. Meth.*, **125**, 225-230 (1975).

9. Ice, G. E., C. J. Sparks, "A simple Cantilevered Mirror for Focussing Synchrotron Radiation", *Nucl. Inst. Meth.*, **A266**, 394-8 (1988).

10. Susini, J., D. Labergerie, "Compact active/adaptive x-ray mirror: bimorph piezoelectric flexible mirror", *Rev. Sci. Instrum.*, **66**, 2229-2231 (1995).

11. Howells, M., "Design strategies for monolithic adjustable-radius metal mirrors", *Opt. Eng.*, **34**, 410-417 (1995).

12. Howells, M. R., D. Lunt, "Design considerations for an ajustable-curvature, high-power, x-ray mirror based on elastic bending", *Opt. Eng.*, **32**, 1981-1989 (1993).

13. Underwood, J. (1994), It has been pointed out by Underwood that the term coma should not be used to describe this aberration and that certain errors beyond mere semantics can result from so doing. However, the usage has become so widespread that it is now conventional. Thus we follow the convention in this work.

14. Ugural, A. C., S. K. Fenster, *Advanced Strength and Applied Elasticity*, Prentice Hall, Englewood Cliffs, 1995.

15. Roark, R. J., W. C. Young, *Formulas for Stress and Strain*, McGraw-Hill, New York, 1975.

16. Timoshenko, S., *Strength of Materials Part II*, Van Nostrand, Toronto, 1940.

17. General Optics, 554 Flinn Ave., Moor Park, CA 93021

18. S. Irick, "Improved measurement accuracy in a long trace profiler", *Nucl. Inst. Meth.*, **A347**, 226-30 (1994).

19. Epoxy glue; Epibond 1210A/9615-10 Ciba Geigy, 5121 San Fernando Rd. West, Los Angeles, CA 90039

Ernest Orlando Lawrence Berkeley National Laboratory
One Cyclotron Road | Berkeley, California 94720

Prepared for the U.S. Department of Energy under Contract No. DE-AC03-76SF00098